Development of kinase inhibitors and activity-based probes

Liu, N.

6 Probing for PKA and AKT1 using photoaffinity probes

N. Liu*, S. C. Stolze*, R. H. Wijdeven, A. W. Tuin, A. M. C. H. van den Nieuwendijk, B. I. Florea, M. van der Stelt, G. A. van der Marel, J. J. Neefjes, H. S. Overkleeft, *Molecular Biosystems*, 2016, **12**, 1809.

6.1 Introduction

The isoquinolinesulfonamide-based kinase inhibitor H-89 (**1**, Scheme 1) was originally identified as a selective and potent inhibitor of protein kinase A (PKA)[1] and has been used to study the role of PKA in various physiological processes.[2] H-89 inhibits PKA in an ATP-competitive manner with the bromocinnamoyl side chain being a crucial factor for the potency and selectivity over other kinases.[3] Though initially presented as a selective PKA inhibitor, H-89 also inhibits a number of other kinases, which is not surprising taking into account that the ATP binding site is

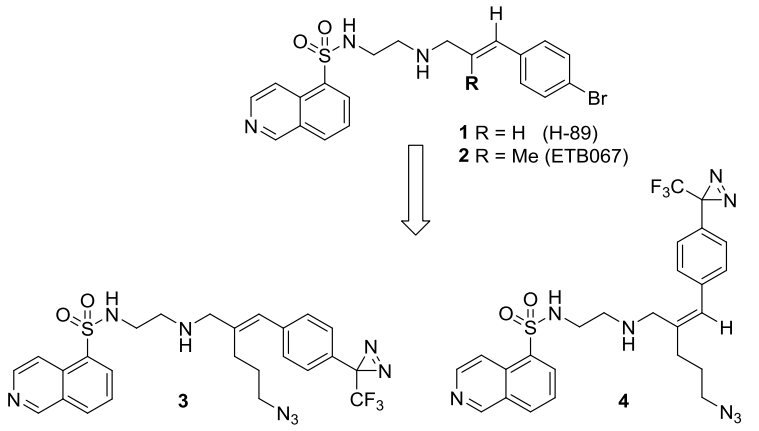

Scheme 1. Structures of the lead compounds: H-89 (**1**) and ETB067 (**2**) and structures of target compounds: diazerine-functionalized photocrosslinking probes **3** (*E*) and **4** (*Z*).

conserved in all kinases.[2,4] PKBα, also referred to as AKT1, is a prominent target of H-89 because of its importance in cancer therapy research. The PI3K/AKT signaling pathway, hyper-activated in many cancer types[5], has effects on vital cellular processes such as survival, metabolism, growth and proliferation.[6] AKT signaling also influences angiogenesis and is involved in metastasis formation via the isoform AKT2. In addition, the PI3K/AKT pathway connects to another critical cell signaling pathway: the Ras/Raf/MEK/ERK signaling cascade.[7] Aside from its involvement in cancer, AKT1 has also been shown to be a key player in bacterial infections by regulation of a network of enzymes essential for the survival of pathogens in phagosomes of host cells. In this context, H-89 and its derivative ETB067 (Scheme 1) were used to distinguish AKT1 from PKA as the crucial enzyme in the control of intracellular bacteria such as *Salmonella typhimurium* and *M. tuberculosis*.[8] AKT1 inhibitors are the first lead antibiotics described that target host proteins rather than bacterial processes.

In the last years, a number of techniques to profile kinases have emerged, such as the kinobead approach that has recently been used to cluster the activity of well-known inhibitors in a kinome-wide screen.[9] Another important technique is capture compound mass spectrometry (CCMS), which is based on combining photo-affinity labeling with biotin-based capture techniques in order to pull-down proteins that bind to an inhibitor and have been covalently captured following photo-affinity labeling. This approach has been used to identify targets of dasatinib, imatinib and staurosporine by converting the inhibitors into capture compounds.[10] The staurosporine capture compound could also be used in comprehensive kinase profiling due to the broad binding profile of staurosporine.[11]

Finally, covalent irreversible kinase inhibitors have received increasing attention both in drug discovery programs and as starting points for kinase bait design. Most of these mechanism-based inhibitors rely on a cysteine thiol in proximity of the binding site that is covalently modified upon binding of the inhibitor.[12] This approach was recently used to target Bruton's tyrosine kinase with Ibrutinib-derived mechanism-based probes.[13] However, not all kinases possess cysteines near the active site, and this holds true as well for PKA and AKT1.[12]
This study aimed at developing a probe derived from H-89 that a) binds efficiently to the target kinases PKA and AKT1; b) contains a photo-activatable group enabling a covalent modification of a captured kinase and c) carries a conjugation handle to attach a reporter moiety such as a fluorophore or biotin using copper-catalysed click chemistry. The studies on H-89 clearly show that the cinnamoyl side chain has an effect on potency and selectivity,[3] so this moiety in the design was kept and the aromatic part of the side chain was modified into an aryl trifluoromethyldiazirine (Scheme 1). Based on the previous studies on ETB067, modification on the double bond of the cinnamoyl system should not have a major influence on activity and therefore a short alkyl chain bearing an azide moiety to enable click labeling has been placed.

6.2 Results and discussion

Synthesis of H-89-based kinase photo-affinity based probes

The synthetic route towards H-89-based photo-affinity based probes **3** and **4** is depicted in Scheme 2. The synthesis commenced from commercially available diethyl cyanomethylphosphonate **5**, which was reacted with trityl-protected bromopropanol **6**[14] to obtain monoalkylated cyanomethylphosphonate **7** in 53% yield. The yield is affected by the fact that dialkylation also occurred, and separation of the two products by column chromatography appeared cumbersome. Before installing the photo-affinity moiety into the probes, trifluoromethylphenyldiazirine functionalised alcohol **8**, which was synthesized by applying a seven step literature procedure[15], was converted into its corresponding aldehyde **9** by Swern oxidation. Next, a Horner-Wadsworth-Emmons (HWE) reaction between *p*-substituted benzaldehyde **9** and phosphonate **7** resulted in α-substituted cinnamonitrile **10** as a 3/2 mixture of *E/Z* isomers in 79% yield. Since separation of the isomers in the nitrile-stage was partially successful, and the nitriles were observed to isomerise during the ensuing transimination, the nitriles were used in the following reaction as an *E/Z* mixture. Subsequently, *E/Z* cinnamonitrile mixture **10** was used in the four-step-one-pot trans-imination

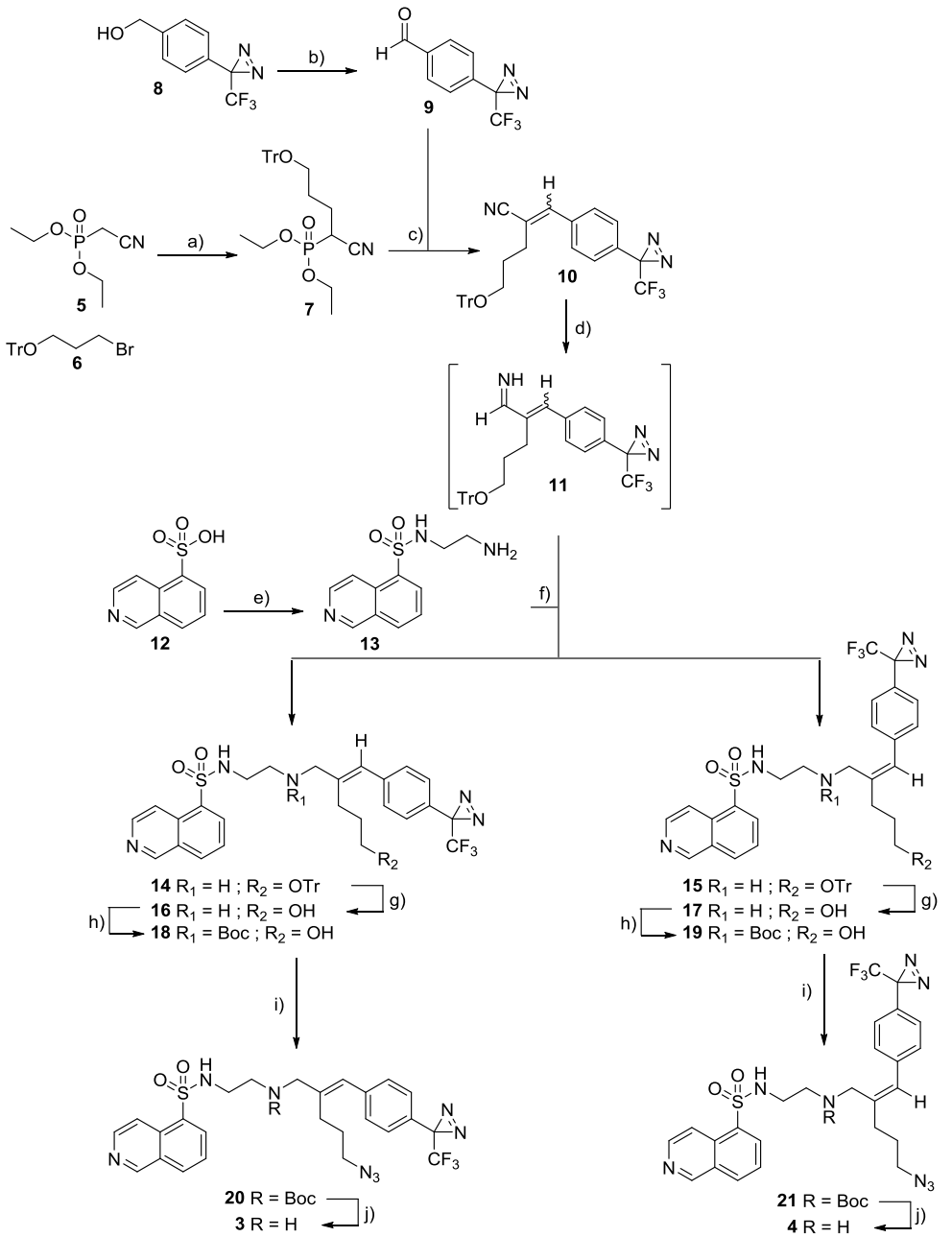

Scheme 2. Reagents and conditions: a) NaH, **6**, 0 °C, DMF, 53%; b) DMSO, $(COCl)_2$, TEA, -78 °C, 89%; c) NaH, **9**, 0 °C, THF, *E/Z* = 3/2, 79%; d) i) DiBAlH, -78 °C, Et_2O/DCM 1:1 v/v; ii) MeOH, -100 °C; e) $SOCl_2$, reflux, DMF; ii) ethylenediamine, DCM, 0 °C, 69%; f) i) **13**, MeOH, RT; ii) $NaBH_4$, -10 °C to RT; ii) TFA, DCM, H_2O; vi) Boc_2O, TEA, DCM, 0 °C, 16% (**18**), 14% (**19**); f) i) TEA, DMAP, TsCl, -20 °C, DCM; ii) NaN_3, DMF, RT, 14% (**20**), 14% (**21**); g) TFA, DCM, RT, 14% (**3**), 14% (**4**).

procedure according to Brussee *et al.*[16], which started with the reduction of nitrile **10** with DiBAlH to form its corresponding aluminated iminium salt intermediate. Excess reagent was then quenched at -100 °C with methanol to obtain the primary imine **11**. The latter was reacted with amine **13**, which was obtained by activating isoquinoline sulfonic amine **12** with thionyl chloride and reacting with ethylenediamine. Next, the resulting secondary imine was reduced by $NaBH_4$ and the crude trityl-protected isoquinolinesulfonamide mixture of **14** and **15** was deprotected under acidic conditions to obtain a crude mixture of **16** and **17** before instalment of the Boc-group to yield isoquinolinesulfonamide **18** and **19** as crude *E/Z* mixture. HPLC purification allowed separation and isolation of both isomers. Both alcohols **18** and **19** were tosylated followed by substitution using NaN_3 to obtain compounds **20** and **21**. At last, deprotection of the Boc-group furnished the photo-affinity based probes **3** and **4** in 14% yield after HPLC purification.

Evaluation of the inhibitory potency and labeling efficiency

With probes **3** and **4** in hand, their biological activity was evaluated. First, the capability of these probes to label a panel of 111 human kinases was examined, which was performed by the company LeadHunter discovery services using a single point kinase active site-directed competition binding Kinome*scan*™ assay (see Chapter 2 for a detailed description)[17]. Briefly, purified recombinant kinases (111 in total) tagged with DNA for qPCR detection are incubated with 10 μM of test compound (here: probe **3** or **4**) and subsequently the mixture of kinases and test compound is transferred to an immobilized ligand that competes with probes for binding to kinases. The results for binding interactions are reported as relative activity percentage, where lower numbers indicate stronger hits in the matrix (Table 1). From Table 1, it can be concluded that the probes **3** and **4** have a preference to inhibit Ser/Thr kinases, since the top ten hits all belong to this family. As expected probe **3**, of which the structure and conformation is most similar to PKA inhibitor H-89 (**1**), inhibits PKA and AKT1 more than its *Z*-analogue **4**. Both probes also inhibited the related kinases AKT2 and AKT3, however at a much lower activity, as also observed for the H-89-derived ETB067 inhibitor.[8]

Table 1. Relative kinase activity compared to control sample (%) after inhibition by compounds **3** and **4** (10 μM).[a]

Kinase	3	4	Kinase	3	4
PKAc-α	1.5	3.4	TAOK1	72	52
AKT1	2.6	18	MEK2	73	72
ROCK2	3	1.7	FAK	74	100
AKT3	3.4	25	VEGFR2	75	85
PRKCH	5	2.8	CLK2	76	72
PRKCE	20	10	JNK1	78	82
PRKCD	23	14	TYK2	78	97
SNARK	23	24	TRKA	79	82
SGK3	31	32	AURKB	80	79
CDK11	35	78	GSK3B	80	74
PRKCI	35	35	PCTK1	80	84
CSNK1D	39	38	JNK3	81	89
MARK3	40	53	FGFR3	82	84
CDK7	43	48	PIK3CG	82	78
DYRK1B	45	74	PLK1	82	83
ALK	50	62	YANK3	82	88
FLT3	50	60	MAPKAPK2	83	95
MLCK	50	76	PIM1	83	81
CSF1R	51	96	ULK2	83	65
TSSK1B	53	56	ZAP70	83	94
AXL	54	74	DYRK1A	84	85
CHEK1	56	72	ERBB4	84	90
SRPK3	57	86	ERN1	85	57
CDK9	58	70	LKB1	85	94
PDGFRB	58	57	PAK4	86	98
PIP5K1A	58	37	ACVR1B	87	100
PDPK1	59	69	p38-beta	87	100
PLK4	59	57	CSNK1G3	89	91
RET	59	76	ERBB2	89	64
FGFR2	60	67	INSR	89	81
KIT	61	70	PAK2	89	96
AMPK-α2	63	83	TGFBR1	89	88
DCAMKL1	63	86	PIM3	90	94
PRKCQ	63	46	AURKA	91	69
EPHA2	65	66	JAK3	91	84
MAP3K4	65	68	PDGFRA	91	98

AKT2	66	91	RAF1	91	78
CDK2	66	92	BMPR2	92	89
CDK3	66	78	PIK3CA	93	94
ABL1-p	67	81	CSNK1G2	94	80
JAK2	67	90	MEK1	95	83
MET	67	55	PAK1	95	95
RSK2	67	72	BTK	96	92
TIE2	68	86	p38-α	96	94
ERK1	69	70	HIPK2	97	95
JNK2	69	86	EGFR	98	100
PLK3	69	73	PIK3C2B	98	94
PIM2	70	62	IKK-beta	99	80
SRC	70	70	MKNK1	99	92
ADCK3	71	96	PIK4CB	99	97
MKNK2	71	71	BRAF	100	93
MST2	71	73	IKK-alpha	100	86
FLT1	72	69	MTOR	100	100
IGF1R	72	63	MYO3A	100	100
MLK1	72	69	RIOK2	100	88
MUSK	72	77			

To further establish the potency of the probes and lead compound H-89 (**1**) for the kinases, PKA, AKT1 and AKT2, their IC_{50} values were determined in a FRET-based assay and their corresponding K_i values were calculated. The results are presented in Table 2.

Table 2. Inhibitory activities of compounds **H-89**, **3** and **4** against PKA, AKT1 and AKT2 (IC_{50} and K_i values in μM).

		PKA	AKT1	AKT2
H89	IC_{50}	1.88 ± 0.64	0.97 ± 0.12	2.47 ± 0.38
	K_i	0.02 ± 0.01	0.09 ± 0.01	1.67 ± 0.26
Probe 3	IC_{50}	75.5 ± 12.54	3.2 ± 1.13	23.1 ± 1.06
	K_i	0.61 ± 0.10	0.02 ± 0.00	0.19 ± 0.09
Probe 4	IC_{50}	74.7 ± 23.12	10.5 ± 4.58	34.4 ± 2.38
	K_i	0.60 ± 0.10	0.04 ± 0.01	0.23 ± 0.03

This kinase assay revealed that probes **3** and **4** are highly potent inhibitors of AKT1 having K_i values varying from 0.02 to 0.04 μM, which are significantly lower than the ones observed for PKA. The trend observed in the Kinomescan for AKT1 is however

preserved with probe **4** being the less potent of the two. A possible explanation for the discrepancy between the assays might be the use of the natural substrate ATP as a competitor to the probes in the FRET-based assay. By comparing the IC_{50} and K_i values of probes **3** and **4** with the lead compound H-89 (**1**), both probes show less activity against PKA, AKT1 and AKT2, but have higher selectivity. Having confirmed the activity of the two probes, a protocol for the photo-labeling of the kinases PKA and AKT1 was designed to validate these compounds as potential photo-affinity based probes.

Using recombinant PKA and AKT1 a robust protocol for the labeling of the kinases with the respective probe was first elucidated, followed by photo-crosslinking at 350 nm, performed in the CaproBox™ system[18] (Caprotec Bioanalytics GmbH, Berlin) and a final click reaction with an alkyne-modified Cy5 reporter for in-gel analysis. Using different concentrations of probe the amounts of probe equivalents required to label the respective kinases was determined. For both PKA and AKT1 5 equivalents of probe (390 nM, PKA; 295 nM AKT1) with respect to the molar amount of kinase were sufficient to label and detect the kinases by in-gel fluorescence (Figure 1, lane 3). Already in these initial experiments it became apparent that probe **3** labels both kinases with a higher affinity than probe **4**, especially in the case of AKT1. The overall stronger labeling of PKA compared to AKT1 can be explained with a higher specific activity of the commercially obtained kinase. The differences in AKT1 labeling are in accordance with the kinetics data. Taking these first results into account, a focus was set on the evaluation of probe **3** in the following experiments.

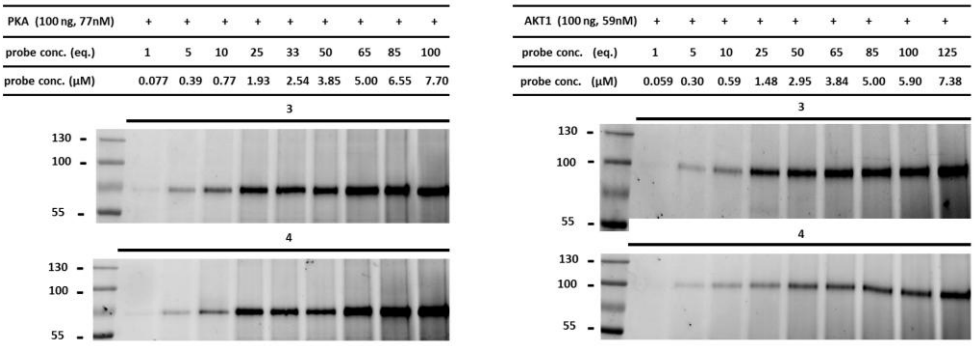

Figure 1. Initial photo-labeling experiments on recombinant kinases using different probe concentrations. Left panel: photolabeling of recombinant PKA using probes **3** and **4**. Right panel: photo-labeling of recombinant AKT1 using probes **3** and **4.**

Subsequently, to prove that the labeling that had been observed in the initial experiments is truly based on affinity to the target kinases and requires active kinases, a number of control experiments have been conducted. First, in order to establish if the labeling is affinity-based, the kinases were mixed with increasing amounts (w/w) of a control protein of similar size and incubated with 5 eq. of **3** (Figure 2, lanes 5-10). The 1:1 controls were also used for further control experiments: one sample was incubated with DMSO and the click mixture to visualize background from association of the proteins with the Cy5 dye (Figure 2, lane 2). A second sample was not irradiated after incubation with the probe, to establish that the UV activation is necessary for labeling (Figure 2, lane 3). Finally, a third sample was denatured by the addition of SDS and subsequent boiling and then treated with the probe to prove that an active enzyme is required for the labeling (Figure 2, lane 4). For both PKA and AKT1 the co-incubation experiment with equivalent amounts of a control protein reveals that the labeling of the targeted kinases with our probes is based on the affinity of the probe towards the target. At higher concentrations of control protein an unspecific reaction of the

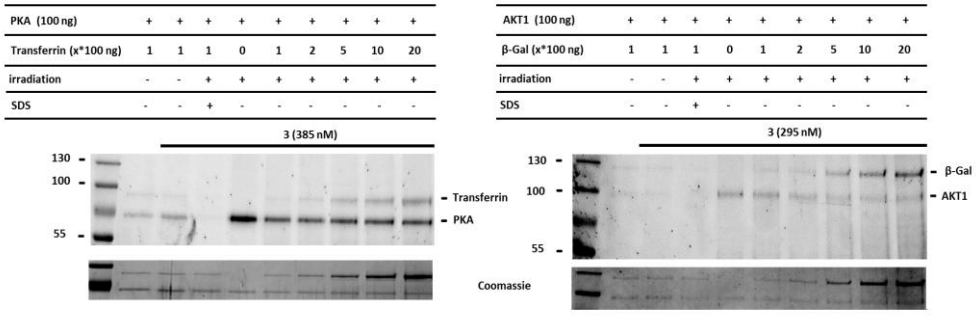

Figure 2. Control experiments using increasing concentrations of Transferrin (PKA, left panel) and β-Galactosidase (AKT1, right panel) as control proteins to determine probe specificity (lanes 5-10). Further controls with 1:1 (w/w) mixtures of kinase and control protein were used to check for background labeling (lane 2), requirement of UV activation (lane 3) and requirement of an active kinase (lane 4).

probe with the control protein and a partial loss of signal for the kinase is observed, especially in the case of AKT1. It has to be noted, that throughout all experiments the labeling of AKT1 was less intense than the labeling of PKA. Since the IC_{50} values that have been determined for both kinases are in the same range for probe **3**, this observation could be explained with different specific activities of the recombinant kinases used in the experiments.

The additional control experiments proved that an active enzyme is indeed required to achieve labeling proven by the disappearance of the labeled kinase when denaturing the sample before incubation with the probe. Also, the labeling relies on UV irradiation proven by the absence of bands in the non-irradiated samples.
In the next set of experiments, competition between **3** and the well-known broad-spectrum kinase inhibitor staurosporine[17] and the parent inhibitors to our probes, H-89 (**1**) and ETB067 (**2**), were visualized. For PKA a very clear competition when pre-incubating with staurosporine was observed, already at 0.5 equivalents to probe **3** (Figure 3, upper panel). For AKT1 a competition is observed as well, however, higher concentrations of staurosporine would be required to achieve full competition (Figure 3, middle panel). Furthermore, the already mentioned lower intensity of labeling for AKT1 not only hampers the visual detection of the competition, it also hinders an accurate quantification by fluorescent densitometry of the bands due to their low intensity (Figure 3, lower panel).

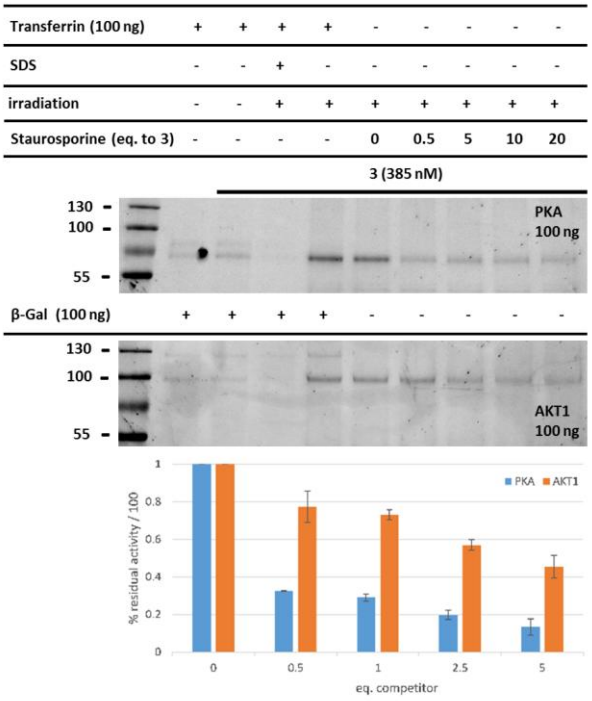

Figure 3 Competition experiments on PKA (upper panel) and AKT1 (middle panel) using Staurosporine as competitor to probe **3**. Quantification of residual activity (lower panel) by fluorescent densitometry from n=3 experiments.

In the competition experiments with H-89 and ETB067, H-89 showed a higher inhibition than ETB067 for both kinases, which is in accordance with previously reported IC_{50} data (Figure 4).[8] For PKA (Figure 4, left panel) a distinct inhibition profile for increasing concentrations of the competitors both in the visual detection of the bands as well as in the quantification of the detected bands was observed. The apparent poorer inhibition of AKT1 can again be explained with the lower signal intensity.

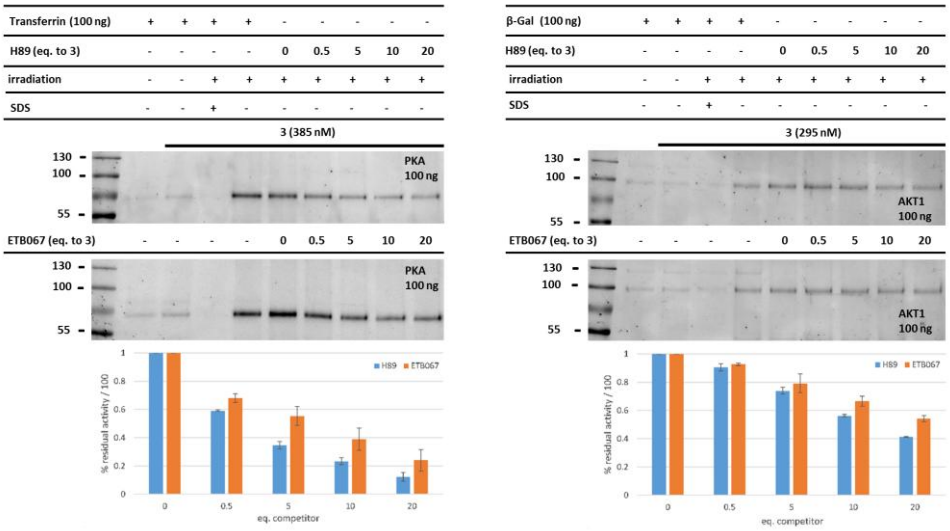

Figure 4 Competition experiments on PKA (left panel) and AKT1 (right panel) using H-89 and ETB067 as competitors to probe **3**. Quantification of residual activity (lower panel) by fluorescent densitometry from n=3 experiments

6.3 Conclusion

Two photo-affinity probes based on the well-known kinase inhibitor H-89 (**1**) have been designed and synthesized. The probes were tested on a panel of kinases and proved to be inhibitors of both PKA and AKT1. Probe **3** has the same double bond geometry as the parent inhibitor H-89 (**1**) and inhibits both PKA and AKT1 with a high potency. A change of the double bond configuration to (*Z*) does not have significant influence on the inhibition of PKA but for AKT1 a partial loss of potency was observed. This indicates a difference in the periphery of the two kinases and offers a possibility to improve selectivity towards AKT1. Furthermore, the efficacy of both probes in the photolabeling of the clinically relevant kinases PKA and AKT1 is shown. The performed experiments however also show that photolabeling conditions need to be adjusted for every new target enzyme. In this study, the

recombinant kinases in pure form as well as in mixtures with control proteins could be labelled; additionally a variety of control experiments reveal that the probes act in an affinity-based manner on active enzymes and that UV activation is required for labeling have been performed. Furthermore, competition experiments with different kinase inhibitors have been performed.

Generating photo-affinity labelled kinase inhibitors is an attractive way to identify other kinase inhibitors and – when used in cell lysates in combination with a conjugation handle – to identify novel inhibitor-novel kinase targets in a relatively unbiased manner. The isolation and identification then have to be improved for reliable detection of targets. This may be achieved by optimizing the probes with *in silico* methods for an optimal placement of the photo-affinity group and the isolation handle. Furthermore, alternative bioconjugation handles could improve the isolation of the targeted kinases.

Experimental

Chemistry

General materials and methods

Tetrahydrofuran (THF) was distilled over $LiAlH_4$ before use. Acetonitrile (ACN), dichloromethane (DCM), *N*,*N*-dimethylformamide (DMF), methanol (MeOH) and trifluoroacetic acid (TFA) were of peptide synthesis grade, obtained from Biosolve, and were used as received. All general chemicals (Fluka, Acros, Merck, Aldrich, Sigma) were used as received. Traces of water were removed from reagents used in reactions that require anhydrous conditions by co-evaporation with toluene. Solvents that were used in reactions were stored over activated 4Å molecular sieves, with the exception of methanol and acetonitrile which were stored over activated 3Å molecular sieves. Unless noted otherwise all reactions were performed under an argon atmosphere. Column chromatography was performed on Silicycle Silia-P Flash Silica Gel, with a particle size of 40 – 63 µm. The eluents toluene and ethyl acetate were distilled prior to use. TLC analysis was conducted on Merck aluminium sheets (Silica gel 60 F254). Compounds were visualized by UV absorption (254 nm), by spraying with a solution of $(NH_4)_6Mo_7O_{24}{\cdot}4H_2O$ (25 g/L) and $(NH_4)_4Ce(SO_4)_4{\cdot}2H_2O$ (10 g/L) in 10% sulphuric acid, a solution of $KMnO_4$ (20 g/L) and K_2CO_3 (10 g/L) in water, or ninhydrin (0.75 g/L) and acetic acid (12.5 mL/L) in ethanol, where appropriate, followed by charring at ca. 150 °C. ^{1}H- and ^{13}C-NMR spectra were recorded on a Bruker DMX-400 (400 MHz) or a Bruker DMX-600 (600 MHz) spectrometer. Chemical shifts are given in ppm (δ) relative to tetramethylsilane (^{1}H-NMR) or $CDCl_3$ (^{13}C-NMR) as internal standard. Mass spectra were recorded on a PE/Sciex API 165 instrument equipped with an Electrospray Interface (ESI) (Perkin-Elmer). High-resolution MS (HRMS) spectra were recorded with a Finnigan LTQ-FT (Thermo Electron). IR spectra were recorded on a Shimadzu FTIR-8300 and absorptions are given in cm^{-1}. Optical rotations $[\alpha]_D23$ were recorded on a Propol automatic polarimeter at room temperature. LC-MS analysis was performed on a

Jasco HPLC system with a Phenomenex Gemini 3 µm C18 50 x 4.6 mm column (detection simultaneously at 214 and 254 nm), coupled to a PE Sciex API 165 mass spectrometer with ESI. HPLC gradients were 10 → 90%, 0 → 50% or 10 → 50% ACN in 0.1% TFA/H_2O. Chiral HPLC analysis was performed on a Spectroflow 757 system (ABI Analytical Kratos Division, detection at 254 nm) equipped with a Chiralcel OD column (150 x 4.6 mm). The compounds were purified on a Gilson HPLC system coupled to a Phenomenex Gemini 5 µm 250 x 10 mm column and a GX281 fraction collector. The used gradients were either 0 → 30% or 10 → 40% ACN in 0.1% TFA/water, depending on the lipophilicity of the product. Appropriate fractions were pooled, and concentrated in a Christ rotary vacuum concentrator overnight at room temperature at 0.1 mbar.

Diethyl (1-cyano-4-(trityloxy)butyl)phosphonate (7)

To an ice-cold solution of NaH (1 eq., 0.20 g, 5.1 mmol, 60% mineral oil) in DMF (15 mL) diethyl cyanomethylphosphonate **5** (0.89 g, 5.0 mmol) was added slowly and allowed to stir for 30 min before addition of ((3-bromopropoxy)methanetrityl) tribenzene **6** (1 eq., 1.94 g, 5.1 mmol). The reaction mixture was allowed to warm to RT and then stirred overnight. The mixture was diluted with H_2O (75 mL) and Et_2O (25 mL), the layers were separated, the aqueous phase extracted with Et_2O (3 x 25 mL) and the combined organic phases were washed with sat. aq. $NaHCO_3$ and brine, dried over $MgSO_4$, filtered and concentrated *in vacuo*. The residue was further purified by silica column chromatography (10% → 50% EtOAc/PE) to afford the title compound as pale yellow oil (yield: 1.27 g, 2.7 mmol, 53%). R_F = 0.3 (50% EtOAc/PE). ^{1}H-NMR (400 MHz, $CDCl_3$, Me_4Si) δ 7.42 (6H, d, *J* = 7.2 Hz, 6 x CH_{ar}), 7.29 (6H, t, *J* = 6.8 Hz, 6 x CH_{ar}), 7.22 (3H, t, *J* = 7.2 Hz, 3 x CH_{ar}), 4.26 – 4.15 (4H, m, 2 x CH_2CH_3), 3.14 (2H, t, *J* = 5.6 Hz, CH_2OCPh_3), 2.95 (1H, ddd, J_1 = 4.8, J_2 = 10.4 Hz, J_3 = 23.2 Hz, CH), 2.12 – 2.00 (1H, m, CH_2-H^a), 1.98 - 1.90 (2H, m, CH_2), 1.84 – 1.75 (1H, m, CH_2-H^b), 1.35 (6H, m, 2 x CH_3). ^{13}C-NMR (101 MHz, $CDCl_3$) δ 143.82, 128.40, 127.66, 126.86, 116.12, 86.47, 63.84, 63.46, 61.91, 30.18, 28.76, 27.74, 24.22, 16.23. HRMS: calculated for $C_{28}H_{32}NO_4P$ $[M+H]^+$ 478.20690; found 478.20372.

4-(3-(Trifluoromethyl)-3H-diazirin-3-yl)benzaldehyde (9)

A solution of DMSO (2.5 eq., 3.22 mL, 45.4 mmol) was cooled to -78 °C and oxalyl chloride (1.3 eq., 2.06 mL, 24.0 mmol) was added dropwise, the reaction mixture was stirred for 30 min at -78 °C. Next, a solution of alcohol **8** (3.93 g, 18.2 mmol) in DCM (10 mL) was added slowly. The reaction was stirred for 1 h at -78 °C before TEA (5 eq., 12.6 mL, 90.8 mmol) was slowly added at -78 °C. The reaction mixture was allowed to warm to 0 °C and was subsequently stirred for 3h. A cold aqueous solution of 20% KH_2PO_4 (50 mL) and cold H_2O (200 mL) was added and the resulting mixture was stirred for 15 min at RT. The mixture was diluted with Et_2O (200 mL) and the layers were separated. The organic layer was washed with a cold aqueous solution of 10% KH_2PO_4 (3 x 50 mL) and brine, dried over $MgSO_4$, filtered and evaporated *in vacuo*. The obtained material was purified by column chromatography (1% EtOAc/PE → 5% EtOAc/PE) and the product was obtained as pale yellow oil (yield: 3.45 g, 16.12 mmol, 89%). ^{1}H-NMR (400 MHz, $CDCl_3$, Me_4Si) δ 10.05 (1H, s, CHO), 7.91 (2H, d, *J* = 8.4 Hz, 2 x CH_{ar}), 7.34 (2H, d, *J* = 8.0

Hz, 2 x CH_{ar}). ^{13}C-NMR (101 MHz, $CDCl_3$) δ 190.85, 136.73, 134.99, 129.65, 126.77, 121.69 (q, *J* = 275.73 Hz), 28.31 (q, *J* = 41.41 Hz). HRMS: calculated for $C_9H_5F_3N_2O$ $[M+H]^+$ 215.03540; found 215.03549.

(*E*/*Z*)-2-(4-(3-(trifluoromethyl)-3*H*-diazirin-3-yl)benzylidene)-5-(trityloxy)pentanenitrile (10)

To an ice-cold suspension of NaH (1.1 eq., 0.64 g, 15.9 mmol, 60% mineral oil) in THF (75 mL) a solution of phosphonate **7** (6.91 g, 14.5 mmol) in THF (25 mL) was added dropwise and stirred for 30 min. Next, a solution of aldehyde **9** (1.1 eq., 3.45 g, 16.6 mmol) in THF (10 mL) was added and the reaction mixture was allowed to warm to RT and stirred overnight. The solution was quenched by addition of freshly prepared sat. aq. Na_2HSO_3 (60 mL) and diluted with H_2O (200 mL) and Et_2O (100 mL). The layers were separated and the aqueous phase was extracted with Et_2O (3 x 100 mL). The combined organic layers were washed with sat. aq. $NaHCO_3$ and brine, dried over $MgSO_4$, filtered and evaporated. The residue was further purified by silica column chromatography (10% → 80% toluene/pentane) to afford the title compound as a white solid with an *E/Z* ratio of 3/2 (yield: 6.16 g, 11.5 mmol, 79%). ^{1}H-NMR (400 MHz, $CDCl_3$, Me_4Si) δ 7.62 (2H, d, *J* = 8.4, 2 x CH_{ar}), 7.42 (6H, d, *J* = 7.2 Hz, 6 x CH_{ar}), 7.27 – 7.15 (11H, m, 11 x CH_{ar}), 6.82 (1H, s, CH), 3.14 (2H, t, *J* = 5.6 Hz, CH_2), 2.55 (2H, t, *J* = 7.2 Hz, CH_2), 1.98 – 1.91 (2H, m, CH_2). ^{13}C-NMR (101 MHz, $CDCl_3$) δ 144.02, 142.03, 134.84, 130.34, 128.71, 128.51, 128.16, 126.94, 126.57, 121.91 (q, 198.97 Hz), 125.24, 118.16, 112.96, 86.46, 61.51, 33.51, 28.23. HRMS: calculated for $C_{33}H_{26}F_3N_3O$ $[M+H]^+$ 538.20280; found 538.20293.

***N*-(2-aminoethyl)isoquinoline-5-sulfonamide (13)**

Isoquinoline-5-sulfonic acid **12** (20.92 g, 100 mmol) was treated with thionylchloride (13 eq., 91.5 mL, 1300 mmol) and a catalytic amount of DMF for 2h at reflux. The reaction mixture was concentrated and the residue was thoroughly washed with DCM before being re-suspended in H_2O (300 mL) at 0 °C. $NaHCO_3$ (1 eq., 8.42 g, 100.2 mmol) was added portion-wise. Next, the mixture was extracted with DCM (3x 500 mL) and dried over $MgSO_4$. The filtrate was added dropwise to a cooled solution of ethylene diamine (5 eq., 33.4 mL, 500 mL) in DCM (250 mL) and the reaction mixture was allowed to warm to RT and stirred for 1h. The mixture was then concentrated before being washed with brine (50 mL). The aqueous layer was extracted with DCM (10 x 50 mL) and the combined organic layers were washed with brine (50 mL), dried over $MgSO_4$, filtered and concentrated. The title compound was obtained as a thick yellow oil (yield: 17.3 g, 69 mmol, 69%) and was used without further purification. ^{1}H-NMR (400 MHz, $CDCl_3$, Me_4Si) δ 9.36 (1H, s, CH_{ar}), 8.67 (1H, d, *J* = 8.4 Hz, CH_{ar}), 8.47 – 8.43 (2H, m, 2 x CH_{ar}), 8.21 (1H, d, *J* = 11.2 Hz, CH_{ar}), 7.71, (1H, t, *J* = 10.0 Hz, CH_{ar}), 3.45 (3H, bs, NH_2 and NH), 3.00 (2H, t, *J* = 5.2 Hz, CH_2), 2.76 (2H, t, *J* = 6.0 Hz, CH_2). ^{13}C-NMR (101 MHz, $CDCl_3$) δ 153.26, 145.06, 133.46, 133.19, 131.23, 129.01, 125.91, 117.22, 45.12, 40.76.

***Tert*-butyl(*E*)-(5-hydroxy-2-(4-(3-(trifluoromethyl)-3*H*-diazirin-3-yl)benzylidene)pentyl)(2-(isoquinoline-5-sulfonamido)ethyl)-carbamate (18)**

A solution of nitrile **10** (3.34 g, 6.2 mmol) in anhydrous Et_2O (20 mL) and DCM (20 mL) was cooled to -78 °C. DiBAl-H (2 eq., 12.4 mL, 12.4 mmol, 1M solution in hexanes) was added dropwise and the reaction

mixture was allowed to warm to 0 °C and stirred for 2h, after which TLC analysis showed complete consumption of the starting material. Next, the mixture was cooled to -100 °C followed by rapid addition of MeOH (13 mL). After 5 min a solution of isoquinoline amine **13** (2.5 eq., 3.90 g, 15.5 mmol) in MeOH (10 mL) was added dropwise and the reaction mixture was allowed to stir at RT overnight. Hereafter, the reaction was cooled to -10 °C and $NaBH_4$ (2 eq., 0.47 g, 12.4 mmol) was added and the mixture was allowed to stir for 4h at RT. The reaction mixture was diluted with 0.5 M aq. NaOH (100 mL) and the layers were separated. The aqueous layer was extracted with DCM (3 x 50 mL) and the combined organic phases were washed with H_2O (3 x 50 mL) and brine, dried over $MgSO_4$, filtered and evaporated. The crude product was subjected to the next step without further purification.

The crude product was dissolved in DCM (20 mL) and TFA (20 mL) was added dropwise. The reaction mixture was stirred for 30 min at RT before addition of H_2O (40 mL), the resulting mixture was stirred for 1h at RT. Hereafter, the mixture was co-evaporated with toluene dissolved in DCM (70 mL) and cooled in an ice bath. To the mixture Boc_2O (1.1 eq., 1.49 g, 6.8 mmol) and TEA (4 eq., 3.4 mL, 24.8 mmol) were added and the reaction was allowed to warm to RT and stirred overnight. The reaction mixture was concentrated under reduced pressure and re-dissolved in H_2O (50 mL) and EtOAc (50 mL). The organic layer was washed with sat. aq. $NaHCO_3$ and brine, dried over $MgSO_4$, filtered and concentrated *in vacuo*. The title compound was obtained after purification by RP-HPLC purification (linear gradient 40% → 60% ACN in H_2O, 0.1% TFA, 15 min) as a yellow oil (yield: 0.61 g, 0.97 mmol, 15.8%).

^{1}H-NMR (400 MHz, $CDCl_3$, Me_4Si) δ 9.32 (1H, s, CH_{ar}), 8.58 (1H, d, *J* = 6.0 Hz, CH_{ar}), 8.39 (1H, d, *J* = 6.4 Hz, CH_{ar}), 8.27 (1H, d, *J* = 7.2 Hz, CH_{ar}), 8.18 (1H, d, *J* = 8.0 Hz, CH_{ar}), 7.65 (1H, t, *J* = 7.6 Hz, CH_{ar}), 7.11 (4H, s, 4 x CH_{ar}), 3.99 (2H, s, CH_2), 3.65 (2H, t, *J* = 6.0 Hz, C*H*$_2$OH), 3.10 (2H, s, CH_2), 2.81 (2H, t, 6.0 Hz, CH_2), 2.09 (2H, t, *J* = 8.0 Hz, CH_2), 1.79 – 1.74 (2H, m, CH_2), 1.39 (9H, s, 3 x CH_3). ^{13}C-NMR (101 MHz, $CDCl_3$) δ 152.94, 144.56, 139.76, 138.19, 134.37, 133.24, 132.80, 131.05, 129.12, 128.87, 127.87, 127.21, 126.10, 125.76, 121.93 (q, *J* = 275.73 Hz), 117.31, 80.78, 61.67, 45.76, 45.31, 41.48, 31.05, 30.06, 28.18 (q, *J* = 40.4 Hz), 28.10. HRMS: calculated for $C_{30}H_{34}F_3N_5O_5S$ $[M+H]^+$ 634.22327; found 634.22333.

Tert-butyl(_Z_)-(5-hydroxy-2-(4-(3-(trifluoromethyl)-3_H_-diazirin-3-yl)benzylidene)pentyl)(2-(isoquinoline-5-sulfonamido)ethyl)-carbamate (19)

This compound was prepared in the same reaction as **18**. The title compound was obtained after purification by RP-HPLC purification (linear gradient 40% → 60% ACN in H_2O, 0.1% TFA, 15 min) as a yellow oil (yield: 0.44 g, 0.7 mmol, 14%). ^{1}H-NMR (400 MHz, $CDCl_3$, Me_4Si) δ 9.31 (1H, s, CH_{ar}), 8.59 (1H, d, *J* = 6.0 Hz, CH_{ar}), 8.45 (1H, d, *J* = 6.4 Hz, CH_{ar}), 8.37 (1H, d, *J* = 6.8 Hz, CH_{ar}), 8.14 (1H, d, *J* = 7.6 Hz, CH_{ar}), 7.60 (1H, t, *J* = 7.6 Hz, CH_{ar}), 7.19 (2H, d, *J* = 8.4 Hz, 2 x CH_{ar}), 7.10 (2H, d, *J* = 8.0 Hz, 2 x CH_{ar}), 6.15 (1H, s, CH), 3.85 (2H, s, CH_2), 3.57 (2H, t, *J* = 6.0 Hz, C*H*$_2$OH), 3.35 (2H, bs, CH_2), 3.12 (2H, t, *J* = 5.6 Hz, CH_2), 2.08 (2H, t, *J* = 7.2 Hz, CH_2), 1.67 (2H, bs, CH_2), 1.40 (9H, s, 3 x CH_3). ^{13}C-NMR (101 MHz, $CDCl_3$) δ 153.01, 144.63, 139.57, 138.33, 134.45, 133.30, 132.95, 131.13,129.16, 128.93, 128.78, 127.16, 126.21, 125.83, 121.98 (q, *J* = 275.73 Hz), 117.41, 61.93, 53.55, 46.41, 42.09, 30.95, 28.22 (q, *J* = 40.4 Hz), 28.15. HRMS: calculated for $C_{30}H_{34}F_3N_5O_5S$ $[M+H]^+$ 634.22327; found 634.22312.

***Tert*-butyl(*E*)-(5-azido-2-(4-(3-(trifluoromethyl)-3*H*-diazirin-3-yl)benzylidene)pentyl)(2-(isoquinoline-5-sulfonamido)ethyl)-carbamate (20)**

Alcohol **18** (0.16 g, 0.26 mmol) was dissolved in DCM (5 mL). After addition of TEA (1 eq., 36 µL, 0.26 mmol) and DMAP (0.64 mg, 5 µmol) the resulting mixture was cooled to -20 °C. A solution of TsCl (1 eq., 0.05 g, 0.26 mmol) in DCM (2 mL) was added dropwise and the reaction was stirred at -20 °C for 18h. Subsequently, 0.1 M aq. HCl (10 mL) was added and the layers were separated. The organic layer was washed with 0.1 M HCl (10 mL) and brine, dried over $MgSO_4$, filtered and concentrated under reduced pressure. The crude product was subjected to the next step without further purification.

The residue was dissolved in DMF (10 mL). To this was added NaN_3 (10 eq., 0.17 g, 2.6 mmol) and the reaction was stirred at room temperature for 5h before being concentrated. The resulting residue was purified by RP-HPLC gradient (linear gradient 40% → 60% ACN in H_2O, 0.1% TFA, 15 min) and the title compound was obtained as light-yellow oil (yield: 0.44 g, 0.7 mmol, 14%). ^{1}H-NMR (400 MHz, $CDCl_3$, Me_4Si) δ 9.36 (1H, s, CH_{ar}), 8.68 (1H, s, CH_{ar}), 8.34 (1H, s, CH_{ar}), 8.29 (1H, d, *J* = 7.2 Hz, CH_{ar}), 8.20 (1H, d, *J* = 8.0 Hz, CH_{ar}), 7.67 (1H, t, *J* = 8.0 Hz, CH_{ar}), 7.16 – 7.09 (4H, m, 4 x CH_{ar}), 6.48 (1H, s, CH), 3.97 (2H, s, CH_2), 3.29 (2H, t, *J* = 6.4 Hz, CH_2N_3), 3.06 (2H, t, *J* = 5.6 Hz, NHCH_2), 2.78 (2H, bs, CH_2), 2.05 (2H, t, *J* = 6.8 Hz, CH_2), 1.78 – 1.75 (2H, m, C$H_2CH_2N_3$), 1.45 (9H, s, 3 x CH_3). ^{13}C-NMR (101 MHz, $CDCl_3$) δ 162.54, 153.14, 145.03, 137.93, 134.30, 133.37, 132.92, 131.11, 129.20, 128.97, 128.73, 127.63, 126.31, 125.74, 122.00 (q, *J* = 275.7 Hz), 117.20, 81.17, 50.82, 45.66, 44.94, 41.87, 30.90, 28.23, 27.43. HRMS: calculated for $C_{30}H_{33}F_3N_8O_4S$ $[M+H]^+$ 659.22976; found 659.22963.

(*E*)-*N*-(2-((5-azido-2-(4-(3-(trifluoromethyl)-3*H*-diazirin-3-yl)benzylidene)pentyl)amino)ethyl)isoquinoline-5-sulfonamide (3)

TFA (0.5 mL) was added to a solution of tert-butyl(*E*)-(5-azido-2-(4-(3-(trifluoromethyl)-3H-diazirin-3-yl)benzylidene)pentyl)-(2-(isoquinoline-5-sulfonamido)ethyl)-carbamate **20** (95 µg, 0.14 mmol) in DCM (0.5 mL). After 1h TLC analysis indicated complete conversion of the starting material. Toluene was added and the mixture was co-evaporated under reduced pressure. In order to remove excess TFA the mixture was co-evaporated twice with toluene. The resulting mixture was purified by RP-HPLC (linear gradient 40% → 60% ACN in H_2O, 0.1% TFA, 15 min) and the title compound was obtained as a yellowish oil (yield: 0.44 g, 0.7 mmol, 14%). ^{1}H-NMR (400 MHz, $CDCl_3$, Me_4Si) δ 9.29 (1H, s, CH_{ar}), 8.57 (1H, d, *J* = 4.8 Hz, CH_{ar}), 8.39 (1H, d, *J* = 5.2 Hz, CH_{ar}), 8.35 (1H, d, *J* = 7.6 Hz, CH), 8.15 (1H, d, *J* = 8.0 Hz, CH_{ar}), 7.64 (1H, t, *J* = 7.6 Hz, CH_{ar}), 7.18 (2H, d, *J* = 8.4 Hz, 2 x CH_{ar}), 7.11 (2H, d, *J* = 8.4 Hz, 2 x CH_{ar}), 6.63 (1H, s, CH), 3.74 (2H, s, CH_2), 3.28 (2H, bs, CH_2N_3), 3.19 (2H, t, *J* = 6.4 Hz, CH_2), 2.33 (2H, t, *J* = 8.4 Hz, CH_2), 1.67 – 1.60 (2H, m, CH_2). ^{13}C NMR (101 MHz, $CDCl_3$) δ 153.96, 144.69, 136.72, 133.95, 133.71, 133.35, 132.62, 131.14, 128.92, 128.85, 128.52, 126.48, 126.03, 121.97 (q, *J* = 274.7 Hz), 177.40, 52.68, 50.70, 46.88, 39.07, 31.17, 28.27 (q, *J* = 41.4 Hz), 26.98, 25.90. HRMS: calculated for $C_{25}H_{25}F_3N_8O_2S$ $[M+H]^+$ 559.17733; found 559.17750.

***Tert*-butyl(*Z*)-(5-azido-2-(4-(3-(trifluoromethyl)-3*H*-diazirin-3-yl)benzylidene)pentyl)(2-(isoquinoline-5-sulfonamido)ethyl)carbamate (21)**

An identical method was used as for the synthesis of tert-butyl(*E*)-(5-azido-2-(4-(3-(trifluoromethyl)-3*H*-diazirin-3-yl)-benzylidene)-pentyl)(2-(isoquinoline-5-sulfonamido)ethyl)-carbamate except that compound **19** (0.39 g, 0.61 mmol) was used as starting material and the amounts of the other reagents were adjusted accordingly. Purification by RP-HPLC (linear gradient 40% → 60% ACN in H_2O, 0.1% TFA, 15 min) yielded the title compound as light yellow oil (yield: 0.44 g, 0.7 mmol, 14%). ^{1}H-NMR (400 MHz, $CDCl_3$, Me_4Si) δ 9.35 (1H, s, CH_{ar}), 8.65 (1H, d, *J* = 6.0 Hz, CH_{ar}), 8.43 (1H, d, *J* = 6.0 Hz, CH_{ar}), 8.39 (1H, d, *J* = 7.2 Hz, CH_{ar}), 8.18 (1H, d, *J* = 8.0 Hz, CH_{ar}), 7.63 (1H, t, *J* = 7.6 Hz, CH_{ar}), 7.19 – 7.13 (4H, m, 4 x CH_{ar}), 6.22 (1H, s, CH), 3.87 (2H, s, CH_2), 3.35 (2H, bs, CH_2N_3), 3.20 (2H, t, *J* = 6.4 Hz, CH_2), 3.11 (2H, bs, CH_2), 2.21 – 2.05 (2H, m, CH_2), 1.67 – 1.63 (2H, m, CH_2), 1.44 (9H, s, 3 x CH_3). ^{13}C-NMR (101 MHz, $CDCl_3$) δ 153.06, 144.79, 138.71, 138.13, 134.41, 133.06, 131.23, 129.20, 128.78, 127.89, 127.56, 126.40, 125.83, 122.04 (q, *J* = 275.7 Hz), 117.37, 81.02, 53.44, 51.33, 46.09, 42.39, 28.24, 27.26, 25.78. HRMS: calculated for $C_{30}H_{33}F_3N_8O_4S$ $[M+H]^+$ 659.22976; found 659.22984.

(*Z*)-*N*-(2-((5-azido-2-(4-(3-(trifluoromethyl)-3*H*-diazirin-3-yl)benzylidene)pentyl)amino)ethyl)isoquinoline-5-sulfonamide (4)

An identical method was used as for the synthesis of **3** except that tert-butyl(*Z*)-(5-azido-2-(4-(3-(trifluoromethyl)-3*H*-diazirin-3-yl)benzylidene)pentyl)(2-(isoquinoline-5-sulfonamido)ethyl)-carbamate (0.56 g, 0.85 mmol) was used as starting material and the amounts of the other materials were adjusted accordingly. Purification by RP-HPLC (linear gradient 40% → 60% ACN in H_2O, 0.1% TFA, 15 min) yielded the title compound as light yellow oil (yield: 0.44 g, 0.7 mmol, 14%). ^{1}H-NMR (400 MHz, $CDCl_3$, Me_4Si) δ 9.46 (1H, bs, CH_{ar}), 8.59 (1H, bs, CH_{ar}), 8.40 (1H, d, *J* = 7.2 Hz, CH_{ar}), 8.31 (2H, d, *J* = 8.0 Hz, 2 x CH_{ar}), 7.76 (1H, t, *J* = 7.6 Hz, CH_{ar}), 7.17 – 7.12 (4H, m, 4 x CH_{ar}), 6.74 (1H, s, CH), 3.82 (2H, s, CH_2), 3.31 (2H, t, *J* = 6.4 Hz, CH_2N_3), 3.12 (2H, s, CH_2), 2.98 (2H, s, CH_2), 2.37 (2H, t, *J* = 7.2 Hz, CH_2), 1.83 – 1.76 (2H, m, CH_2). ^{13}C-NMR (101 MHz, $CDCl_3$) δ 150.45, 139.88, 136.78, 135.16, 134.62, 134.33, 133.80, 132.40, 132.15, 128.93, 128.59, 127.54, 126.77, 121.94 (q, *J* = 275.7 Hz), 119.69, 50.55, 46.71, 45.73, 38.87, 31.13, 31.07, 28.20 (q, *J* = 40.4 Hz), 26.98. HRMS: calculated for $C_{25}H_{25}F_3N_8O_2S$ $[M+H]^+$ 559.17733; found 559.17753.

Biochemistry

IC_{50} and K_i determination by FRET assay

Kinase activity was measured using a FRET-based assay with a peptide from ribosomal protein S6 as substrate. 10 nM ULight-rpS6 peptide (Perkin-Elmer) was incubated with 100 µM ATP and 2 nM Eu-labeled anti-phospho-rpS6 antibody (Perkin-Elmer, recognizing pSer S6 at position 235 and 236) in HEPES buffer (50 mM HEPES pH 7.5, 1 mM EGTA, 10 mM $MgCl_2$, 2 mM DTT and 0.01% Tween-20) together with 0.5 nM/min AKT1 or 0.05 nM/min PKA (SignalChem), in the presence or absence of the probe or H-89. During incubation at RT, the intensity of the light emission was measured with intervals of 60 min on a

PE Envision reader using the Lance Ultra kinase assay settings (λ_{ex} 320 nm; λ_{em} 665 nm) and a secondary control emission was measured at 615 nm. In control experiments, no ATP was added to the buffer. Data was analyzed using GraphPad Prism 5 (GraphPad software, La Jolla, USA).

To determine the K_M for the kinases, the same assay was performed using a fixed concentration of probe or H-89 (2µM) and 0, 0.1, 0.2, 0.5, 1, 2, 5, 10, 20, 50, 100, 200, 500, 1000 µM ATP. K_M values were calculated using GraphPad Prism 5 (GraphPad software, La Jolla, USA).

K_i values were calculated via equation 1.1:

$$K_i = IC_{50} / (1 + ([S]/K_M)) \quad (1.1)$$

where K_i is the inhibition constant, IC_{50} is the half maximal inhibitory concentration, S is the concentration of substrate and K_M is the Michaelis-Menten constant, which is the substrate concentration at which the reaction rate is half maximum. All experiments were conducted in triplicate and curves were corrected for background fluorescence of the solvent.

Photo-labeling of recombinant kinases (PKA, AKT1)

PKA (PKAc beta) and AKT1 were purchased from Signalchem, aliquoted, stored at -80 °C and thawed only once for an experiment.

For pre-denatured samples the solutions were treated with 10% SDS (2 µL) and boiled for 5 min before addition of the probes. Non-irradiated samples were protected from light by wrapping in aluminium foil. Competition experiments were performed in triplicate, quantification of residual activity was achieved by fluorescent densitometry using the Biorad Image Lab software (version 5.2.1).

In a typical experiment, 100 ng (1 µL [100 ng/µL] of recombinant enzyme were added to the assay buffer (17 µL) (20 mM HEPES, pH 7.5, 50 mM KCl, 10 mM $MgCl_2$, 10% glycerol)(adapted). For competition experiments, the respective inhibitor (1 µL, 20X) was added next and the samples were incubated in the dark at RT for 30 min. For all experiments probe **3**, probe **4** (2 µL, 10X or 1 µL, 20X in competition experiments) or DMSO were added and the samples were incubated for 30 min at RT in the dark. For irradiation the samples were transferred to a clear, flat-bottom 96-well plate and diluted with 30 µL 100 mM HEPES, pH 7.5. The samples were then irradiated for 5 min at 0 °C and transferred back into Eppendorf tubes, the concentration was further adjusted by adding 5 µL of 100 mM HEPES, pH 7.5; the untreated samples were diluted in the same way. For the attachment of the Cy5 fluorophore by click reaction samples were treated with "click mix" (6 µL/sample), prepared freshly as follows: 3 µL 25 mM $CuSO_4$ (aq.) were mixed with 1.8 µL 0.25 M sodium ascorbate, resulting in a brown solution, this was then vortexed until a colour change to bright yellow was achieved, indicating the reduction of the copper ion. Next, THPTA (0.6 µL, 25 mM in DMSO) was added and the mixture vortexed again. Finally, 0.6 µL of a 150X Cy5 alkyne (relative to the amount of probe used in the experiment) was added, the mixture vortexed again, added to the sample, mixed and incubated for 1h at RT in the dark. The final concentrations of the click reagents were 1.25 mM $CuSO_4$, 7.5 mM sodium ascorbate, 250 µM THPTA

and 1.5 eq. Cy5 alkyne. The reaction was stopped by adding 20 µL of SDS loading buffer and boiling for 5 min.

Samples were resolved by 10% SDS-PAGE, for in-gel detection of fluorescent bands, wet gel slabs were scanned with ChemiDoc MP system using Cy5 settings.

References

[1] T. Chijiwa, A. Mishima, M. Hagiwara, M. Sano, K. Hayashi, T. Inoue, K. Naito, T. Toshioka and H. Hidaka, *J. Biol. Chem.*, 1990, **265**, 5267.

[2] A. Lochner and J. A. Moolman, *Cardiovasc. Drug Rev.*, 2006, **24**, 261.

[3] R. A. Engh, A. Girod, V. Kinzel, R. Huber and D. Bossemeyer, *J. Biol. Chem.*, 1996, **271**, 26157.

[4] S. P. Davies, H. Reddy, M. Caivano and P. Cohen, *Biochem. J.*, 2000, **351**, 95.

[5] J. A. Engelmann, *Nat. Rev. Cancer*, 2009, **9**, 550.

[6] B. D. Manning and L. C. Cantley, *Cell*, 2007, **129**, 1261.

[7] K. Moelling, K. Schad, M. Bosse, S. Zimmermann and M. Schweneker, *J. Biol. Chem.*, 2002, **277**, 31099.

[8] C. Kuijl, N. D. L Savage, M. Marsman, A. W. Tuin, L. Janssen, D. A. Egan, M. Ketema, R. van den Nieuwendijk, S. J. F. van den Eeden, A. Geluk, A. Poot, G. van der Marel, R. L. Beijersbergen, H. Overkleeft, T. H. M. Ottenhoff and J. Neefjes, *Nature*, 2007, **450**, 725.

[9] G. Médard, F. Pachl, B. Ruprecht, S. Klaeger, S. Heinzlmeir, D. Helm, H. Qiao, X. Ku, M. Wilhelm, T. Kuehne, Z. Wu, A. Dittmann, C. Hopf, K. Kramer and B. Kuster, *J. Proteome Res.*, 2015, **14**, 1574.

[10] J. F. Fischer, C. Dalhoff, A. K. Schrey, O. Y. Graebner, S. Michaelis, K. Andrich, M. Glinski, F. Kroll, M. Sefkow, M. Dreger and H. Koester, *J. Proteomics*, 2011, **75**, 160.

[11] J. F. Fischer, O. Y. Graebner, C. Dalhoff, S. Michaelis, A. K. Schrey, J. Ungewiss, K. Andrich, D. Jeske, F. Kroll, M. Glinski, M. Sefkow, M. Dreger and H. Koester, *J. Proteome Res.*, 2010, **9**, 806.

[12] T. Barf and A. Kaptein, *J. Med. Chem.*, 2012, **55**, 6243.

[13] N. Liu, S. Hoogendoorn, B. van der Kar, A. Kaptein, T. Barf, C. Driessen, D. V. Filippov, G. A. van der Marel, M. van der Stelt and H. S. Overkleeft, *Org. Biomol. Chem.*, 2015, **15**, 5147.

[14] US Pat., US20080096903(A1), 2008.

[15] M. Wiegand and T. K. Lindhorst, *Eur. J. Org. Chem*, 2006, 4841.

[16] A. M. C. H. van den Nieuwendijk, A. B. T. Ghisaidoobe, H. S. Overkleeft, J. Brussee and A. van der Gen, *Tetrahedron*, 2004, **60**, 10385-10396.; P. Zandbergen, A. M. C. H. van den Nieuwendijk, J. Brussee and A. van der Gen, *Tetrahedron*, 1992, **48**, 3977.

[17] M. W. Karaman, S. Herrgard, D. K. Treiber, P. Gallant, C. E. Atteridge, B. T. Campbell, K. W. Chan, P. Ciceri, M. J. Davis, P. T. Edeen, R. Faraoni, M. Floyd, J. P. Hunt, D. J. Lockhart, Z. V. Milanov, M. J. Morrison, G. Pallares, H. K. Patel, S. Pritchard, L. M. Wodicka and P. P. Zarrinkar, *Nat. Biotech.*, 2008, **26**, 127.

[18] Y. Luo, C. Blex, O. Baessler, M. Glinksi, M. Dreger, M. Sefkow and H. Koester, *Mol. Cell. Proteomics*, 2009, **8**, 2843.